

ORIGINAL ARTICLE

Mouse model of NASH that replicates key features of the human disease and progresses to fibrosis stage 3

Kristy St. Rose¹ | Jun Yan^{2,3} | Fangxi Xu^{4,5}  | Jasmine Williams¹ |
 Virginia Dweck¹ | Deepak Saxena^{4,5} | Robert F. Schwabe² |
 Jorge Matias Caviglia^{1,2} 

¹Department of Health and Nutrition Sciences, Brooklyn College, CUNY, New York, New York, USA

²Department of Medicine, Columbia University, New York, New York, USA

³Department of Forensic Medicine, Medical College of Nantong University, Nantong, Jiangsu, China

⁴Department of Molecular Pathobiology, New York University College of Dentistry, New York, New York, USA

⁵Department of Surgery, New York University School of Medicine, New York, New York, USA

Correspondence

Jorge Matias Caviglia, Department of Health and Nutrition Sciences, Brooklyn College, CUNY, 2900 Bedford Ave., Brooklyn, NY 11210, USA.
 Email: jorgem.caviglia@brooklyn.cuny.edu

Funding information

National Cancer Institute, Grant/Award Number: K22CA178098, P30CA013696 and R01CA206105; National Institute of Dental and Craniofacial Research, Grant/Award Number: R01DE025992; National Institute of Diabetes and Digestive and Kidney Diseases, Grant/Award Number: R01DK128955 and R03DK101863; National Institute on Aging, Grant/Award Number: R01AG068857; National Natural Science Foundation of China, Grant/Award Number: NSFC81300346

Abstract

Nonalcoholic fatty liver disease (NAFLD) is the most common liver disease in the United States and the world; with no Food and Drug Administration–approved pharmacological treatment available, it remains an area of unmet medical need. In nonalcoholic steatohepatitis (NASH), the most important predictor of clinical outcome is the fibrosis stage. Moreover, the Food and Drug Administration recommends that clinical trials for drugs to treat this disease include patients with fibrosis stage 2 or greater. Therefore, when using animal models for investigating the pathophysiology of NAFLD and for the preclinical evaluation of new drugs, it is important that the animals develop substantial fibrosis. The aim of this study was to develop a mouse model of NAFLD that replicated the disease in humans, including obesity and progressive liver fibrosis. Agouti yellow mutant mice, which have hyperphagia, were fed a Western diet and water containing high-fructose corn syrup for 16 weeks. Mice became obese and developed glucose intolerance. Their gut microbiota showed dysbiosis with changes that replicate some of the changes described in humans with NASH. They developed NASH with activity scores of 5–6 and fibrosis, which was stage 1 after 16 weeks, and stage 3 after 12 months. Changes in liver gene expression assessed by gene-set enrichment analysis showed 90% similarity with changes in human patients with NASH. **Conclusion:** Ay mice, when fed a Western diet similar to that consumed by humans, develop obesity and NASH with liver histology, including fibrosis, and gene expression changes that are highly similar to the disease in humans.

Kristy St. Rose and Jun Yan contributed equally to this work.

This is an open access article under the terms of the [Creative Commons Attribution-NonCommercial-NoDerivs](https://creativecommons.org/licenses/by-nc-nd/4.0/) License, which permits use and distribution in any medium, provided the original work is properly cited, the use is non-commercial and no modifications or adaptations are made.

© 2022 The Authors. *Hepatology Communications* published by Wiley Periodicals LLC on behalf of American Association for the Study of Liver Diseases.

INTRODUCTION

Nonalcoholic fatty liver disease (NAFLD) has become the most common chronic liver disease in the United States and the world.^[1] Although the initial form of NAFLD, nonalcoholic fatty liver (NAFL), is considered benign, the most advanced form, nonalcoholic steatohepatitis (NASH), which affects a third of patients, can progress to cirrhosis, end-stage liver disease, and hepatocellular carcinoma.^[2] Treatment of NASH includes weight loss through diet and exercise, which has been shown to ameliorate NASH; however, weight loss is difficult to achieve and maintain.^[3] As an alternative, several drugs have been tested for the treatment of NASH.^[4] Although pioglitazone, vitamin E, and obeticholic acid have shown to improve NASH in clinical trials, no treatment has been approved by the Food and Drug Administration (FDA),^[5–7] and the FDA considers NASH with fibrosis or cirrhosis an area of unmet medical need.^[8]

Mechanistic and preclinical studies of new drugs for the treatment of NAFLD need animal models that replicate the characteristics of the disease in humans. Although many models have been described, there is no model considered optimal and widely adopted for studying NAFLD.^[9–12] In particular, several models of NASH show little or no fibrosis. Because mice do not develop liver fibrosis easily, in some models, fibrosis was induced using a diet deficient in choline and methionine or the administration of carbon tetrachloride.^[9–13] However, those approaches do not necessarily replicate the pathophysiology of NAFLD in humans. The presence of substantial fibrosis and how fibrosis is induced are important points, as fibrosis stage has been consistently shown to be the best predictor of mortality in patients with NASH.^[14–16] Moreover, both the FDA and the European Medicines Agency recommend that clinical trials of drugs for the treatment of NASH include patients with fibrosis stages 2 or higher.^[8,17]

An optimal animal model of NAFLD would replicate the characteristics of NAFLD in humans. First, the model should show pathophysiology, progression, and histological features similar to those described in humans.^[10,13] Second, the animals should develop obesity and related systemic alterations, as NASH and obesity are closely related, particularly in Western countries.^[1] Finally, these alterations should be induced by factors that commonly play a role in the development of NAFLD in humans, such as excessive food intake, diets high in fat and simple carbohydrates, and/or low physical activity.

In this article, we report the characterization of a mouse model of NAFLD induced by feeding hyperphagic, agouti yellow (Ay), mice with a Western diet and a solution containing high-fructose corn syrup. The mice develop NASH with fibrosis, which is stage 1 after 16 weeks and stage 3 after 12 months, as well

as dysbiosis, and gene-expression changes similar to those described in humans.

EXPERIMENTAL PROCEDURES

Animals and diets

We used mice carrying the agouti yellow mutation (Ay mice) and their wild-type littermates. Experimental mice were produced by breeding male Ay mice (B6.Cg-Ay/J; Jackson #000021) and female C57BL/6J mice (Jackson #000664); the background strain of all mice was C57BL/6J. Experimental mice were male. Mice were fed either a Western diet, containing fat (42 kcal%), cholesterol (0.2% wt/wt) and sucrose (341 g/kg) (Envigo TD.88137), or a control diet with low fat (13 kcal%) and sucrose (120 g/kg) (Envigo TD.08485). Mice fed the Western diet also received a drinking solution containing 42 g/L of a mixture of fructose and glucose (55% and 45%, respectively, equal to 23 g/L of fructose and 19.1 g/L of glucose) (Sigma F2543 and 49,159); the solution was sterile-filtered and replaced weekly/semiweekly. Mice were fed the diets starting at 8 weeks of age, and for either 12 weeks, 16 weeks, or 12 months. Cage bedding was wood chips. Mice were group-housed under specific pathogen-free or conventional conditions. Mice were on a 12-h/12-h light/dark cycle; sample were collected during the light cycle. Mice were fasted for 5 to 6 h before sample collection and euthanized with carbon dioxide. Mice were assigned consecutive identification numbers that were used during sample analyses, which were conducted blind. All animals received humane care according to the criteria outlined in the Guide for the Care and Use of Laboratory Animals; protocols were approved by the Columbia University or Brooklyn College Institutional Animal Care and Use Committee.

Evaluation of liver steatosis, injury, inflammation, and fibrosis

For histological evaluation, formaldehyde-fixed, paraffin-embedded liver sections were stained using hematoxylin and eosin (H&E), Masson's trichrome, and picosirius red. Sections were evaluated, and grade and stage were determined by a pathologist experienced in liver diseases (J.Y.), using the NASH–Clinical Research Network criteria.^[18] Liver triacylglycerol (TAG) content was determined by extracting lipids and quantifying TAGs using the Infinity Triglycerides Reagent (Thermo Fisher Scientific; TR22421).^[19] Liver injury was evaluated by measuring plasma alanine aminotransferase (ALT) and aspartate aminotransferase (AST) activities (BQ-Kits BQ004A; GenWay GWB-BQK284). Fibrosis was quantified both morphometrically and by

quantifying hydroxyproline, as detailed in the supplemental material and previously described.^[20]

RESULTS

Ay mice fed a diet high in fat and fructose develop obesity and glucose intolerance

To induce obesity and NASH with fibrosis in a relatively short period of time, we used mice carrying the Agouti yellow (A^y) mutation, which causes hyperphagia by blocking melanocortin 4 receptors (MC4R) in the hypothalamus.^[21,22] Interestingly, MC4R mutations are the most common cause of monogenic obesity, and MC4R polymorphisms have been linked to polygenic obesity in human populations.^[23,24] Melanocortin receptors are expressed at extremely low levels (for MC1R) or not expressed (for MC2R to MC5R) in the liver; therefore, it is unlikely that the Ay mutation has any direct effect in the liver (Table S1). Ay mice develop obesity, insulin resistance, and other alterations related to the metabolic syndrome; thus, they have been used extensively as models for those diseases.^[21]

Ay mice were fed a Western diet and a drinking solution containing fructose to mimic the intake of high-fructose corn syrup-sweetened beverages.^[25,26] This combination of food and drinking solution provides 49 kcal% of carbohydrates, 35 kcal% of fat, and 16 kcal% of proteins, which is similar to the mean macronutrient composition of diets in the United States.^[27] We designated this diet as high-fat and fructose diet (HFFD) and we refer to these mice as Ay-HFFD (Table 1). Wild-type C57BL/6 mice (WT) fed a control low-fat and fructose diet (LFFD) were included as lean controls and designated as WT-LFFD. In addition, we included a group of Ay mice fed the LFFD (Ay-LFFD) and a group of wild-type C57BL/6 male mice fed the HFFD diet (WT-HFFD). Mice were fed these diets starting at 8 weeks of

age, and for 16 weeks. As expected, caloric intake was higher in hyperphagic Ay mice than in WT mice fed the same diet, and intake was also higher in mice fed the HFFD compared with those fed the LFFD (Figure S1A).

Ay mice fed the LFFD (Ay-LFFD), WT mice fed the HFFD diet (WT-HFFD), and Ay mice fed the HFFD diet (Ay-HFFD) gained more weight than the WT mice fed the LFFD diet (WT-LFFD), which were used as controls; Ay-HFFD mice nearly doubled their body weight (Figure 1A). Weight gain was mostly due to increased adipose tissue, as shown by increased fat pad weight (Figure 1B; Figure S1B–D) and greater total body fat mass (Figure 1C). Leptin was elevated in Ay-HFFD mice when compared with control (WT-HFFD) mice (Figure S1E).

WT-HFFD and Ay-HFFD mice developed glucose intolerance, as assessed by glucose tolerance tests, with significantly higher glycemia at 60 and 120 min after glucose administration, and greater areas under the curve (Figure S1F,G). Moreover, Ay-LFFD, WT-HFFD, and Ay-HFFD showed increased insulin (Figure S1H).

In summary, Ay mice fed LFFD, WT mice fed the HFFD, and Ay mice fed the HFFD for 16 weeks developed obesity, and WT and Ay mice fed the HFFD also developed glucose intolerance and hyperinsulinemia, replicating metabolic alterations characteristics of the metabolic syndrome and associated with NAFLD.^[3]

Ay mice fed the HFFD develop NASH with fibrosis

Livers from Ay-LFFD, WT-HFFD, and Ay-HFFD mice fed the diets for 16 weeks were enlarged compared with those from WT-LFFD mice, and had a light yellowish color characteristic of steatosis (Figure 2A). WT-HFFD and Ay-HFFD mice developed hepatomegaly, with greater liver weights and liver-to-body weight ratios that

TABLE 1 Experimental groups

	Group designation			
	WT-LFFD	Ay-LFFD	WT-HFFD	Ay-HFFD
Genotype	WT	Ay	WT	Ay
Hyperphagia	No	Yes	No	Yes
Diet	LFFD	LFFD	HFFD	HFFD
Steatosis	–	–/+	+++	+++
Injury	–	–	++	++
Inflammation	–	–/+	+	++
Fibrosis	–	–	–	+
NAFLD stage	Normal (controls)	Normal or NAFL or NASH	NASH	NASH + fibrosis

Note: Genotype, diets, designation, and main characteristics of experimental groups after 16 weeks of diet feeding. Minus and plus signs indicate absence or presence and relative degree of each alteration.

Abbreviation: NAFL, nonalcoholic fatty liver.

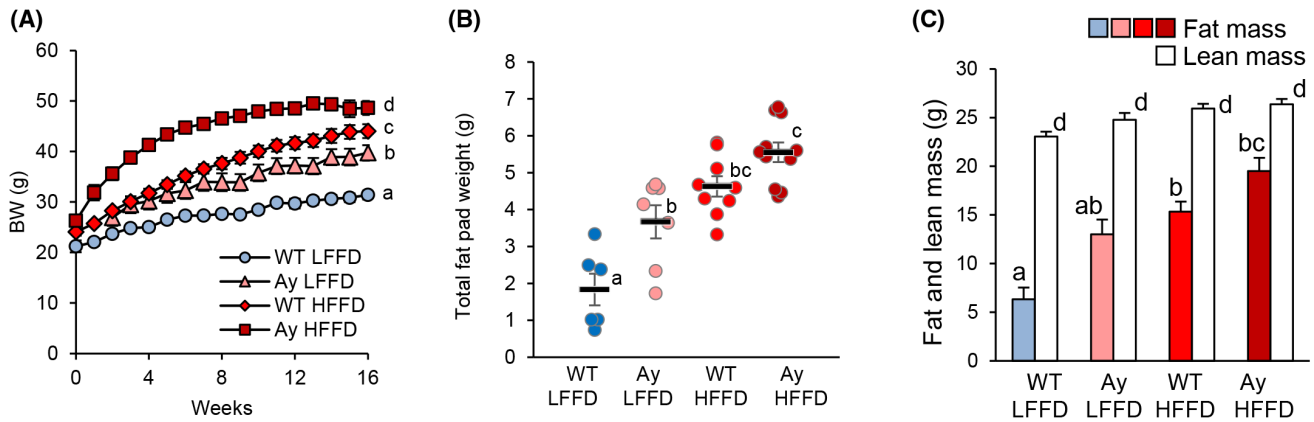


FIGURE 1 Agouti yellow (Ay) mice fed a low-fat and fructose diet (LFFD), wild-type (WT) mice fed a high-fat and fructose diet (HFFD), and Ay mice fed a HFFD developed obesity after 16 weeks of diet feeding: body weight (BW; A); total weight of main fat pads (sum of perigonadal, inguinal, and perirenal fat pad weights) (B); total body fat mass measured by nuclear magnetic resonance (color bars represent fat mass; white bars represent lean body mass, which did not significantly differ between groups) (C). Data represent the mean and SEM; $N = 6, 7, 11$; 11 animals per group in the order shown in the graphs. Statistical analysis was done by analysis of variance (ANOVA) and Tukey *post-hoc* test; letters next to the data points or bars that are different indicate groups that are significantly different with $p < 0.05$.

were higher than in controls (WT-LFFD) (Figure 2B; Figure S2A).

Histological evaluation and scoring of H&E-stained sections showed that both groups of mice fed the HFFD diet, WT-HFFD and Ay-HFFD, developed steatosis, ballooning, and inflammation, the main characteristics of NASH (Table 2, Figure 2C). Ay-LFFD mice had variable grades of steatosis, with no significant differences in ballooning or inflammation when compared with controls (Table 2). Control WT-LFFD mice had NAFLD activity scores (NAS) of 1, considered normal; Ay-LFFD mice had scores of about 3, whereas WT-HFFD and Ay-HFFD mice had scores of about 6, which commonly correspond to NASH (Figure 2D).^[18] Indeed, none of the WT-LFFD mice, 57% of the Ay-LFFD, and 100% of both the WT-HFFD and the Ay-HFFD mice showed the combination of steatosis, ballooning, and inflammation, which is considered diagnostic for NASH.^[18,28]

Ay-LFFD, WT-HFFD, and Ay-HFFD mice showed hepatic steatosis, which was panacinar and mixed macrovesicular and microvesicular (Figure 2C; Table 2). Steatosis was quantified by measuring the liver content of triacylglycerol, which was increased both in WT-HFFD and Ay-HFFD mice when compared with WT-LFFD (Figure 2E).

Hepatocyte injury, evaluated by the presence of ballooning in H&E-stained sections, was minimal in WT-LFFD and Ay-LFFD mice. In contrast, both WT-HFFD and Ay-HFFD mice showed ballooning (Table 2). Hepatocyte injury was confirmed by measuring plasma ALT and AST, which were increased in WT-HFFD mice and to a higher level in Ay-HFFD mice (Figure 2F; Figure S2B).

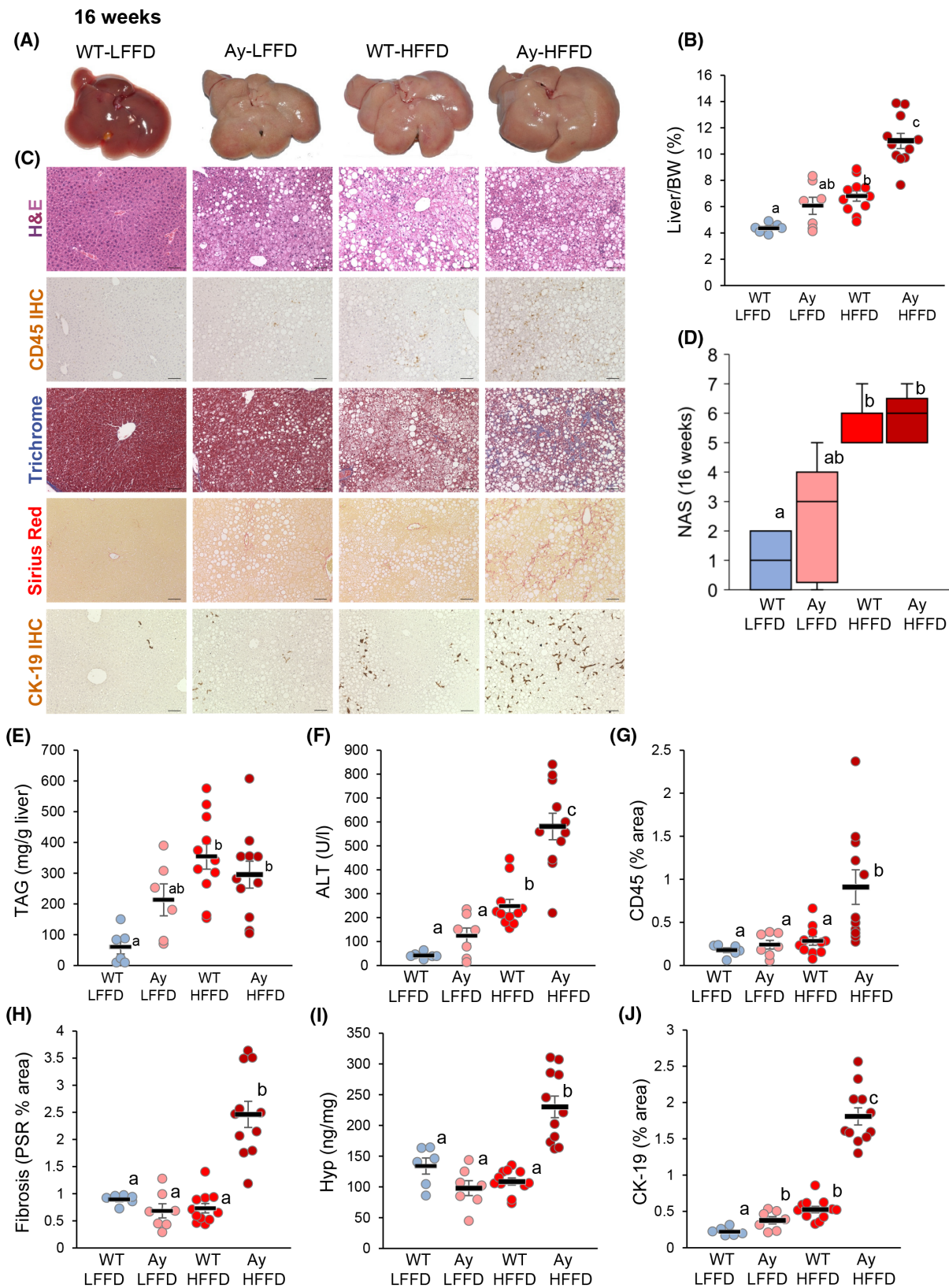
Inflammation scores were increased in WT-HFFD and Ay-HFFD diet (Table 2). Ay-HFFD mice had increased liver infiltration with inflammatory cells, as shown by CD45 immunohistochemistry staining

(Figure 2C,G). Moreover, Ay-LFFD, WT-HFFD, and Ay-HFFD mice all showed increased liver messenger RNA (mRNA) expression of genes encoding for cytokines tumor necrosis factor alpha (TNF α) and C-C motif chemokine ligand 2 (CCL2), and the inflammatory receptor toll-like receptor 4 (TLR4) (Figure S2C–E).

Because fibrosis is the best predictor of outcome in NASH,^[14,16] we evaluated whether these mice developed fibrosis. Ay mice fed the HFFD for 16 weeks showed fibrosis by picrosirius red and Masson's trichrome staining (Figure 2C). Fibrosis for Ay-HFFD mice fed the diet for 16 weeks was stage 1, significantly greater than in WT-LFFD controls (Table 2). Importantly, fibrosis was pericellular, reproducing the typical pattern found in early stages of NASH-induced fibrosis.^[29] Morphometric quantification of collagen in picrosirius red–stained sections confirmed that fibrosis was greater in Ay-HFFD mice compared with controls (Figure 2H). Quantification of collagen by measuring the hepatic hydroxyproline content further confirmed that Ay-HFFD mice had increased fibrosis (Figure 2I). In addition, Ay-HFFD mice showed extensive ductular reaction, which has been shown to correlate with the grade of liver fibrosis in patients with NASH (Figure 2C,J).^[30]

Ay mice, when fed the HFFD for 12 weeks, did not show histological fibrosis (data not shown), supporting the idea that, in these mice, 16 weeks of diet treatment are necessary for the development of fibrosis.

When fed the diets for 12 months, most Ay-LFFD, WT-HFFD, and Ay-HFFD mice developed NASH (Table 3), with NASH Activity Scores between 4 and 7 (Figure 3C). They showed hepatomegaly with liver steatosis (Table 3; Figure 3A,B, and D). At 12 months, Ay-LFFD, WT-HFFD, and Ay-HFFD mice had hepatocellular injury and inflammation (Table 3; Figure 3A,E, and F). Therefore, after 12 months, Ay-LFFD, WT-HFFD, and Ay-HFFD had NASH. More importantly,



Ay-LFFD and WT-HFFD mice showed fibrosis stage 2 and Ay-HFFD mice showed fibrosis stage 3 (Table 3). Fibrosis was quantified by picosirius red staining of collagen and measurement of hydroxyproline liver

content, with both methods showing that WT-HFFD and Ay-HFFD mice had greater fibrosis than the WT-LFFD controls (Table 3; Figure 3A,G, and H). Therefore, in this model, over time, fibrosis progresses

FIGURE 2 Ay-LFFD, WT-HFFD, and Ay-HFFD mice developed various stages of NAFLD (16 weeks). (A) Macroscopic images of livers after 16 weeks. (B) Liver-to-body weight ratios. (C) Representative $\times 100$ microscopic images of livers stained with hematoxylin and eosin (H&E), CD45 by immunohistochemistry (IHC; inflammatory infiltration), trichrome, picrosirius red (PSR) stainings (fibrosis), and cytokeratin 19 (CK-19) by IHC (ductular reaction) ($\times 100$ images, bars = 100 μm). (D) Nonalcoholic fatty liver disease (NAFLD) activity scores (NAS). (E) Triacylglycerol content (TAG) of livers. (F) Plasma alanine aminotransferase (ALT). (G) CD45 immunohistochemistry quantification. (H) Morphometric quantification of fibrosis in PSR-stained sections. (I) Hydroxyproline (Hyp) content of livers. (J) CK-19 IHC quantification. Scatter plots found in (B) and (E)–(J) show individual data points, means, and SEM. Box and whisker plot found in (D) shows the median (midline) and interquartile range, and whiskers indicate maximum and minimum values ($N = 6, 7, 11,$ and 11 per group). Different letters indicate significant differences with $p < 0.05$ (ANOVA and Tukey *post-hoc* test in [B] and [E]–[J]) or ANOVA on ranks in [D]).

TABLE 2 NAFLD histological grades and stages (16 weeks)

Features	WT-LFFD	Ay-LFFD	WT-HFFD	Ay-HFFD
Steatosis	0 (0, 1) ^a	1.5 (0, 2) ^{a,b}	3 (2, 3) ^b	3 (2, 3) ^b
Ballooning	0 (0, 0.5) ^a	0.5 (0, 1) ^a	2 (2, 2) ^b	2 (2, 2) ^b
Inflammation	0 (0, 0) ^a	1 (0.75, 1) ^{a,b}	1 (1, 1) ^b	1 (1, 2) ^b
Fibrosis	0 (0, 0) ^a	0 (0, 1) ^a	0 (0, 1) ^a	1 (1, 1) ^b

Note: NAFLD was evaluated using the NASH–Cancer Research Network (CRN) scoring system. Grade and stage data are expressed as median (with first and third quartiles). Different superscript letters indicate statistically significant differences ($p < 0.05$ by Kruskal-Wallis ANOVA on ranks).

TABLE 3 NAFLD histological grades and stages (12 months)

Features	WT-LFFD	Ay-LFFD	WT-HFFD	Ay-HFFD
Steatosis	0 (0, 1.5) ^a	3 (3, 3) ^b	2 (2, 3) ^b	2 (2, 2) ^b
Ballooning	1 (0, 1) ^a	2 (2, 2) ^a	1 (1, 1.75) ^a	1 (1, 2) ^a
Inflammation	1 (0.5, 1) ^a	1 (1, 2) ^a	1 (1, 1) ^a	1 (1, 1) ^a
Fibrosis	1 (1, 1) ^a	2 (2, 2) ^{ab}	2.5 (2, 3) ^{b,c}	3 (3, 3.75) ^{b,c}

Note: NAFLD was evaluated in mice fed the diets for 12 months using the NASH-CRN scoring system. Data are expressed as median (with first and third quartiles). Different superscript letters indicate statistically significant differences ($p < 0.05$ by Kruskal-Wallis ANOVA on ranks).

to advanced stages, similarly to the course of the disease in human patients. In Ay-LFFD, WT-HFFD, and Ay-HFFD, plasma ammonia and total bilirubin were similar to controls, indicating that the liver function was preserved (not shown).

To further investigate the NASH-associated fibrosis, we assessed the number and activation of hepatic stellate cells (HSCs), the main cell type responsible for fibrosis in NASH.^[31] To evaluate the number of HSCs, we used a gene signature that we have previously developed to identify HSCs in single-cell RNA-sequencing data from mouse livers, which consists of genes highly expressed selectively in HSCs.^[32] We used this HSC signature to interrogate transcriptional profiles from the livers of the WT-LFFD, Ay-LFFD, WT-HFFD, and Ay-HFFD mice. All genes in the HSC signature, including *Des* (desmin), *Lrat* (lecithin retinol acyltransferase), and *Pdgfrb* (platelet-derived growth factor beta) genes, were induced in livers from Ay-HFFD mice, indicating an increase in the number of HSCs (Figure S3A). We confirmed the increase in mRNA expression of desmin, a classical marker of HSCs, by quantitative polymerase chain reaction (PCR) (Figure S3B). Desmin expression, evaluated by immunohistochemistry, appeared to be

more prominent in the areas of liver with macrovesicular steatosis (Figure S3C).

To assess the activation of HSCs, we used a gene signature characteristic of activated liver myofibroblasts, which in liver derive predominantly from HSCs.^[31,32] Expression of most of the genes included in the gene signature was increased in liver from Ay-HFFD mice compared with controls (Figure S3D). Moreover, livers of Ay-HFFD and WT-HFFD showed increased mRNA expression of fibrosis markers *Acta2* (smooth muscle actin alpha 2), *Col1a1* (collagen type I alpha 1 chain), *Lox* (lysyl oxidase), and *Timp1* (tissue inhibitor of metalloproteinase 1), which are expressed primarily by activated HSCs (Figure S3E,G–I). In addition, Ay-HFFD mouse livers showed expression of α -SMA (smooth muscle actin) by immunohistochemistry, in contrast to undetectable or minimal expression in control WT-LFFD mice (Figure S3F).

In summary, WT and Ay mice fed the HFFD diet for 16 weeks developed NASH that closely replicates the alterations described in humans. More importantly, Ay mice fed the HFFD for 16 weeks showed HSC activation and fibrosis deposition with readily quantifiable collagen, which progressed to stage 3 after 12 months.

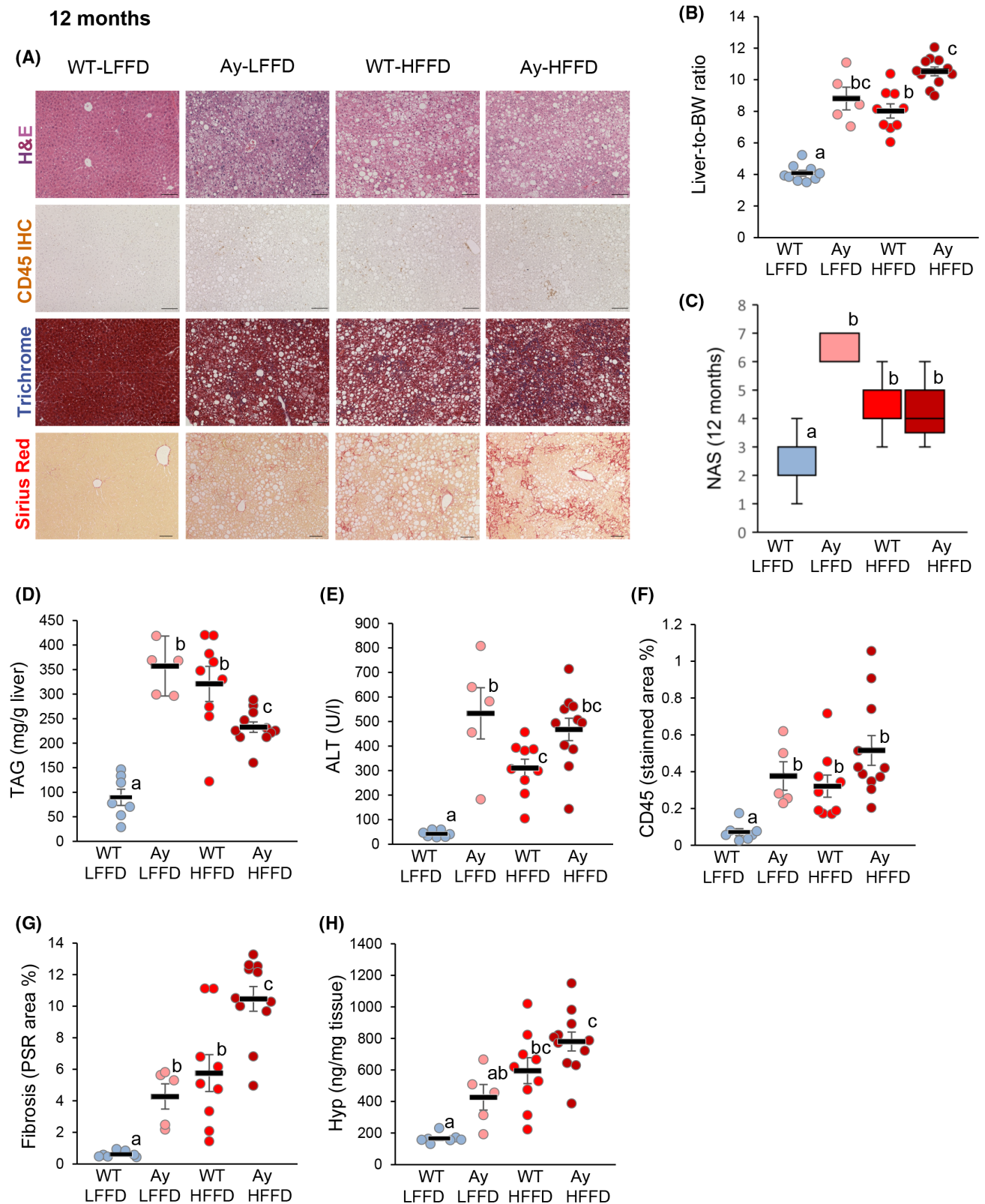


FIGURE 3 Ay-LFFD, WT-HFFD, and Ay-HFFD mice developed NASH with fibrosis (12 months). (A) Representative $\times 100$ microscopic images of livers stained with H&E, CD45 by IHC (inflammatory infiltration), trichrome, and PSR stainings (fibrosis) ($\times 100$ images, bars = $100\ \mu\text{m}$). (B) Liver-to-body weight ratios. (C) NAS. (D) Triacylglycerol content of livers. (E) Plasma ALT. (F) CD45 IHC quantification. (G) Morphometric quantification of fibrosis in PSR-stained sections. (H) Hydroxyproline content of livers. Scatter plots (panels [B] and [D]–[H]) show individual data points, means, and SEM. Box and whisker plot found in (C) show the median (midline) and interquartile range, and whiskers indicate maximum and minimum values ($N = 7, 5, 9,$ and 11 per group). Different letters in (C) indicate significant differences with $p < 0.05$ (ANOVA and Tukey *post-hoc* test in [B] and [D]–[H] or ANOVA on ranks in [C]).

Ay mice fed the HFFD show gut microbiota dysbiosis

Because NAFLD has been associated with gut microbiota dysbiosis,^[33] to evaluate the gut microbiota in our mice, we collected cecum content and determined its bacterial composition by 16S ribosomal RNA sequencing.

Principal coordinate analysis of beta diversity at the operational taxonomic unit level of mice fed the diets for 16 weeks showed differences in microbial communities across experimental groups (Figure 4A). Microbiota in Ay-HFFD mice was significantly different from the microbiota in control WT-LFFD, suggesting that in Ay-HFFD mice, NASH was associated with dysbiosis of the gut microbiota (Figure S4A). The microbiota from Ay-HFFD mice showed richness similar to WT-LFFD (but higher than for Ay-LFFD), as assessed by alpha diversity measures Chao1 and ACE indices, whereas diversity evenness across the groups was similar based on the Shannon and Simpson index measurements (Figure S4B,C). At the phylum level, Ay-HFFD mice showed nonstatistically significant trends toward higher abundance of Bacteroidetes and its major genus, *Bacteroides* (Figure 4B; Figure S4D). In addition, Ay-HFFD mice showed a decrease in Tenericutes and TM7/Saccharibacteria when compared with WT-LFFD (Figure 4B; Figure S4E,F). For these last two phyla, abundance progressively decreased in experimental groups with more advanced stages of NAFLD, with the greatest change in Ay-HFFD mice. In addition, when analyzed at the genus level, Ay-HFFD mice showed decreased *Ruminococcus* when compared with Ay-LFFD (Table S2).

In summary, Ay-HFFD mice show changes in their gut microbiota composition when compared with

controls, which can be characterized as dysbiosis and include changes that replicate some of the alterations described in human patients with NASH.^[34]

Ay mice fed the HFFD show gene-expression patterns characteristic of NASH

To determine whether the alterations in hepatic gene expression in this model were similar to those in human NASH, we generated hepatic transcriptional profiles in our mice fed the diets for 16 weeks. Although Ay-LFFD and WT-HFFD mice showed more moderate changes, the Ay-HFFD mice showed greater changes in liver gene expression when compared with the WT-LFFD control mice (Figure 5A). These changes agree with Ay-HFFD mice having the most pronounced histological and biochemical liver alterations, and Ay-LFFD and WT-HFFD showing intermediate changes (Figure 2). Ay-HFFD mouse livers showed induction of lipogenic genes (*Acaca* [acetyl-CoA carboxylase alpha], *Fasn* [fatty acid synthase], *Scd1* [stearoyl-CoA desaturase 1], *Scd2*, *Cd36* [clusters of differentiation 36], and peroxisome proliferator-activated receptor gamma [*Pparg*]), inflammation genes (*Tnf*, *Ccl2*, *Saa1* [serum amyloid A1], and *Tlr4*), and fibrosis-related genes (*Col1a1*, *Lox*, and *Timp1*), which is consistent with the histological alterations and changes in mRNA measured by quantitative PCR (Figure 2; Figure S2C–E; Figure S3G–I).

Gene-set enrichment analysis (GSEA) against the Hallmark gene-set collection using GSEA showed that 25 gene sets (pathways) were significantly enriched in Ay-HFFD mice when compared with controls (out of 50 gene sets in the nonredundant Hallmark collection) (Table S3). Ay-LFFD and WT-HFFD mice showed

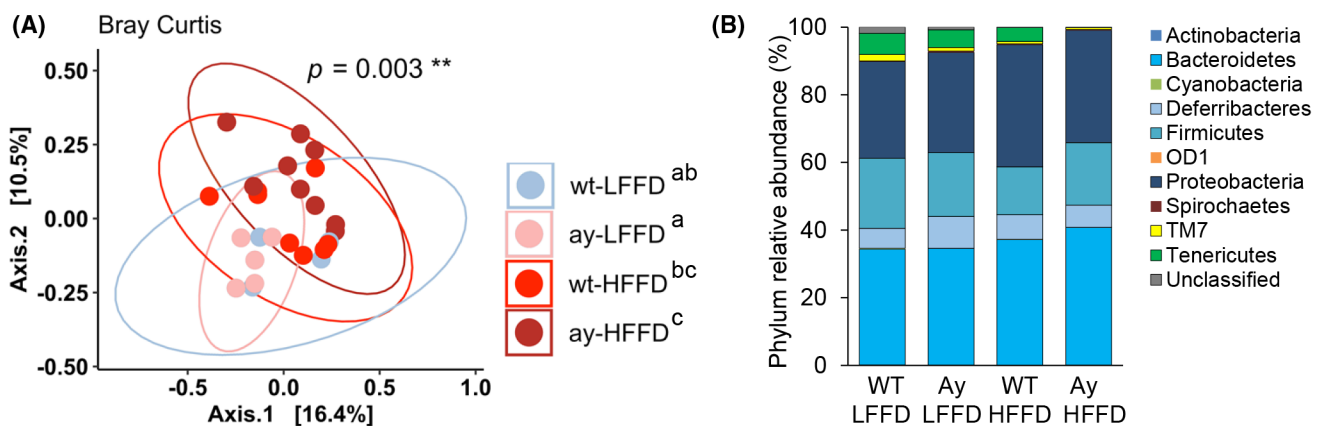


FIGURE 4 Nonalcoholic steatohepatitis (NASH) development is associated with gut microbiota dysbiosis. (A) Principal coordinates analysis based on Bray Curtis dissimilarity matrix comparing all experimental groups; different superscripts in the legend indicate statistically significant differences based on permutational multivariate ANOVA ($p < 0.05$). (B) Gene-set enrichment analysis (GSEA) of Ay-HFFD versus WT-HFFD mouse livers, showing the 10 gene sets with the highest scores. (C) Composition of the gut microbiota at the phylum level (as relative abundance) shows microbiota changes in WT-HFFD and Ay-HFFD mice. In both panels, $N = 4, 5, 8, \text{ and } 9$, in the order shown in (B).

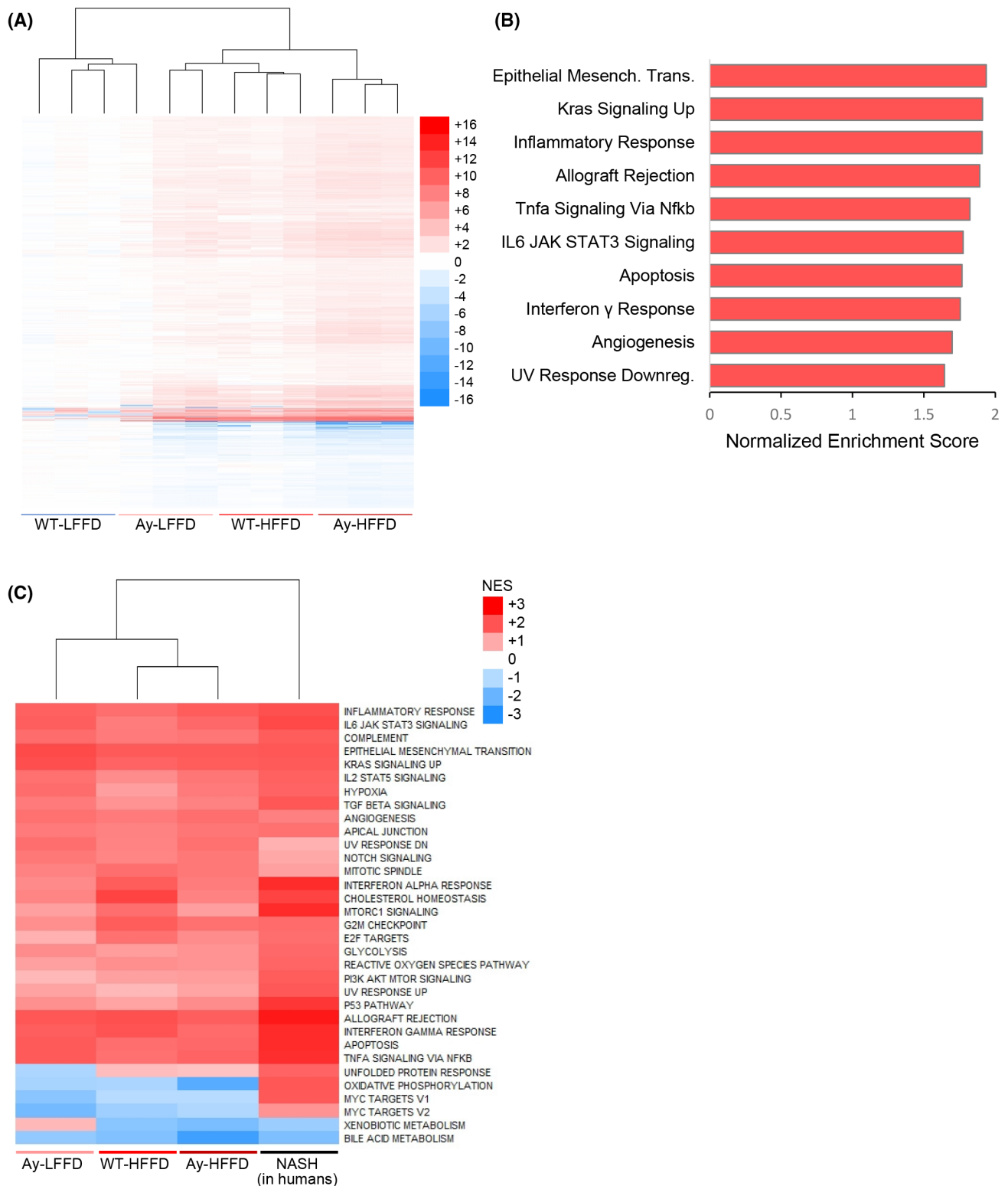


FIGURE 5 Gene expression in livers from mice with NAFLD and comparison to humans. (A) Transcriptional profiles of livers ($N = 3$ per group). (B) Comparison of GSEA in livers from mice and human patients with NASH; heatmap represents normalized enrichment scores ($N = 3$ per group for mouse samples and 45 for human NASH; gene sets included had a family-wise error rate < 0.05 in GSEA in at least one mouse group or in the human data). IL, interleukin; NfKb, nuclear factor kappa B; STAT3, signal transducer and activator of transcription 3; TGF, tumor growth factor; Tnfa, tumor necrosis factor alpha.

enrichment in 21 and 23 gene sets, respectively. The gene sets with the highest scores in Ay-HFFD included those related to apoptotic cell death (apoptosis pathway), inflammation (inflammatory response, allograft rejection, TNF α signaling, interleukin-6–JAK–signal transducer and activator of transcription 3 signaling, and interferon gamma response), and fibrosis (epithelial mesenchymal transition, which in Ay-HFFD liver was driven by high expression of genes such as *Col1a1*, *Col1a2*, *Lum* [Lumican], and *Mmp2* [matrix metalloproteinase 2]). These gene sets correspond to processes that are important in the pathogenesis of NASH (Figure 5B).^[35,36] Importantly, comparison of gene sets enriched in these mice and those enriched in human patients with NASH^[37] showed that of the gene sets that were significantly enriched in at least one group, 90% (30 gene sets out of 33) were analogously up-regulated or down-regulated in livers of both Ay-HFFD mice and human patients with NASH (Figure 5C).

Therefore, gene-expression analysis indicates that this mouse model of NASH replicates most changes in gene expression that occur in human patients with NASH, suggesting that the molecular mechanisms associated to NAFLD development in this model are similar to those in humans.

DISCUSSION

We have developed a mouse model of NASH by feeding hyperphagic Ay mice with a combination of a Western diet and high-fructose corn syrup–containing water, which replicates the average US diet. These mice develop obesity, gut microbiota dysbiosis, and NASH with fibrosis that closely resemble the human disease in its histology and liver gene-expression changes.

Although mice fed a high-fat diet can develop obesity and NASH, these mice often do not develop liver fibrosis, at least in periods of 4 months or shorter, and mice are considered to be relatively resistant to developing fibrosis.^[13] To induce NASH with fibrosis, researchers have used the classical methionine and choline-deficient diet, choline-deficient high-fat diets, diets with high content of trans fats, and diets containing very high amounts fructose, saturated fat, and cholesterol.^[9,10,13] Although these diets are effective in inducing NASH in mice, their composition is not found in human diets, and some of them do not cause obesity or insulin resistance.^[9] Diets deficient in choline, such as the methionine choline–deficient diet, cause rapid weight loss, and choline-deficient high-fat diets prevent mice from gaining weight; this may not replicate the pathophysiology of NASH, as most patients with NASH are obese.^[10] Diets with very high content of fat and cholesterol are uncommon for humans, and trans fats are being eliminated from foods. Therefore, models of

NASH driven by diets often do not fully replicate the characteristics of the disease in humans.

To try to replicate human diets, we selected a Western diet that was originally developed to induce atherosclerosis, and we combined it with high-fructose corn syrup,^[26] which results in a macronutrient composition that is similar to the average US diet.^[27] Moreover, this diet is a subtype of the high-fat, high-fructose diets that have been reported to best replicate human NASH.^[9] However, when fed to WT mice for 16 weeks, this diet causes obesity and NASH, but no fibrosis, as seen in our WT-HFFD mice; these mice may develop fibrosis only after 6 to 12 months.^[26] To accelerate the development of fibrosis, we used the hyperphagic Ay mice, which, when fed the HFFD, developed NASH with fibrosis that is stage 1 after 16 weeks, and progresses to stage 3 after 1 year. Hyperphagic MC4R-deficient mice have also been used to induce NASH.^[38] However, in those mice, the MC4R deficiency is driven by a floxed transcriptional block sequence upstream of MC4R, which can be removed by the Cre recombinase. Therefore, use of the Cre-lox system for tissue-specific gene deletion will result in the unwanted re-expression of MC4R in Cre-targeted tissues, which can lead to confounding effects.

The FDA considers that treatments for NASH with fibrosis are likely to have the greatest impact on clinical outcomes, and recommends that clinical trials include patients with fibrosis stages 2 or 3.^[8] Although inducing NASH in mice is relatively easy, the development of fibrosis, which is a marker of progression and prognosis in humans, is more difficult to achieve.^[13] Several mouse models have been reported to induce NASH with fibrosis^[10,11,13]; however, they also have certain disadvantages: The methionine choline–deficient diet induces liver fibrosis, but it also causes nutritional deficiency and weight loss, which is the opposite of the obesity often found in humans with NASH. The DIAMOND model also shows fibrosis, but the particular genetic background would require backcrossing for use with genetically modified strains.^[39] Finally, the administration of a high-fat diet in combination with CCl₄ has been reported to result in development of fibrosis in only 12 weeks; however, in this “diet- and chemical-induced” model, the chemical hepatotoxicity has no parallel in human NASH.^[13,40] Our model provides an additional alternative: Ay-HFFD mice develop fibrosis, which was initially stage 1 (16 weeks), and progressed to stage 3 (12 months), similar to the disease progression in humans. Although the 12 months needed for Ay-HFFD to develop stage 3 fibrosis is a considerable time, we consider it reasonable to speculate that pharmacological treatments that prevent stage 1 fibrosis at 16 weeks are likely to reduce the stage 3 fibrosis found at 12 months as well.

NAFLD is associated with gut microbiota dysbiosis, which has been proposed to be involved in

NAFLD development and progression.^[33,41] Although Ay-HFFD mice show a trend toward an increase in Bacteroidetes, which is similar to changes reported in patients with NASH,^[34,42,43] the lack of statistically significance may be due to the small samples size. Interestingly, the decrease in Rominococcus in Ay-HFFD is similar to the decrease described in patients with NASH and advanced fibrosis.^[34,43] Therefore, this model of NASH shows similarities to the changes in patients with NASH.

Transcriptional profiling allows for a comprehensive unbiased evaluation of disease-related changes in gene expression, which can be associated with pathophysiological mechanisms. GSEA of transcriptional data from the liver of Ay-HFFD mice showed activation of the main processes that contribute to the pathogenesis of NASH and associated signaling pathways. These include apoptosis, the main mechanism of hepatocyte cell death, multiple inflammatory pathways, and epithelial mesenchymal transition, associated with fibrosis. The similarity in hepatic GSEA between Ay-HFFD mice and humans with NASH suggests that this mouse model replicates most of the disease mechanisms active in humans; therefore, this model of NASH can be used for studying the pathogenesis of NASH, therapeutic targets, and to test potential drugs. However, our analysis points to changes in a few gene sets that are not common to both species (Myc targets, β -oxidation), suggesting that this model is not optimal for the study of those mechanisms.

In summary, this model has several advantages. First, NASH with fibrosis is induced with a diet that is similar to the average US diet and that does not require non-physiological amounts of nutrients such as trans fats or cholesterol, induction of nutritional deficiencies (such as the choline-deficient diets) or administration of hepatotoxins such as CCL₄.^[9,13,44] Second, mice develop liver fibrosis that is quantifiable both morphometrically and by measuring the hydroxyproline liver content. Third, this model allows for the study of different stages of NAFLD. We describe three combinations of mouse genotypes and diets that can result in different stages of NAFLD: After 16 weeks, Ay-LFFD mice develop NAFL or mild NASH; WT-HFFD develop NASH; and Ay-HFFD develop NASH with fibrosis (Table 1). Alternatively, different stages of NAFLD can be induced in the same mice by extending the treatment period, as our three groups of obese mice developed NASH with fibrosis after a year. Fourth, the Ay mutation is dominant, which allows for more efficient breeding when compared with mutations that require homozygosity (MC4RKO or ob/ob).^[38,45] In addition, the Ay mutation confers a yellow coat color; therefore, mutant mice can easily be identified by phenotype without the need for genotyping.^[46] Fifth, Ay mice are commercially available in the C57BL6/J strain, which is

commonly used for obesity and metabolic studies, and is the most common background for transgenic mice, thus not requiring backcrossing. Finally, in this model, deletion of TLR4 decreased fibrosis (unpublished data), as described in other models of liver fibrosis, showing that this model is useful for studying the pathophysiology of NASH.^[47,48]

This model also has a few limitations. Induction of NASH in WT mice and NASH with fibrosis in Ay mice takes 16 weeks; although still a considerable time, it is relatively shorter than with other NASH models.^[10,12,13] To obtain development of NASH-induced fibrosis, we used mice carrying the Ay mutation. It may be preferable to study NASH in WT mice; however, WT mice are relatively resistant to the development of fibrosis. The Ay mutation does not appear to have major effects on the liver, as melanocortin receptors are not or minimally expressed in liver and because the transcription profiles of livers from Ay-LFFD and Ay-HFFD do not cluster together (Figure 5). In addition, the mutation does not appear to directly cause NASH or fibrosis, because on the one hand, Ay mice fed a low-fat diet do not develop fibrosis until after 12 months, and on the other hand, WT mice also develop NASH with fibrosis when fed the same diet (HFFD) for a longer period (1 year). Therefore, using Ay mice allows us to accelerate the progression of the disease, but fibrosis development is not directly caused by the Ay mutation.

CONCLUSION

We developed and characterized a method to induce NASH with fibrosis in mice using a diet similar to human diets, which results in alterations that closely resemble the development of the disease in humans.

AUTHOR CONTRIBUTIONS

Experiments and data analysis: Kristy St. Rose, Jasmine Williams, Virginia Dweck, and Jorge Matias Caviglia. *Histology sample analysis:* Jun Yan. *Microbiome data analysis:* Fangxi Xu and Deepak Saxena. *Study advice and manuscript review:* Robert Schwabe. *Study design and supervision, data collection and interpretation, and manuscript draft and review:* Jorge Matias Caviglia.

ACKNOWLEDGMENT

We thank Silvia Affo and Xinyin Jiang for the helpful discussions, Kathleen Axen and Amy Marcinkiewicz for reviewing the manuscript, Ajay Nair for advice on bioinformatics, and Enrique Pouget for advice on statistics.

FUNDING INFORMATION

Supported by the National Institutes of Health (K22CA-178098, R03DK101863, R01DK128955, R01CA-206105, DE025992, and R01AG068857); Brooklyn College; National Natural Science Foundation of China

(NSFC81300346); National Institutes of Health/National Cancer Institute Cancer Center (P30CA013696); and the Columbia University Genomics and High Throughput Screening Shared Resource.

CONFLICT OF INTEREST

D.S. owns Periomics Care LLC.

ORCID

Fangxi Xu  <https://orcid.org/0000-0002-4265-2133>

Jorge Matias Caviglia  <https://orcid.org/0000-0002-5880-6459>

REFERENCES

1. Younossi Z, Anstee QM, Marietti M, Hardy T, Henry L, Eslam M, et al. Global burden of NAFLD and NASH: trends, predictions, risk factors and prevention. *Nat Rev Gastroenterol Hepatol*. 2018;15:11–20.
2. Brunt EM. Nonalcoholic steatohepatitis: definition and pathology. *Semin Liver Dis*. 2001;21:3–16.
3. Chalasani N, Younossi Z, Lavine JE, Charlton M, Cusi K, Rinella M, et al. The diagnosis and management of nonalcoholic fatty liver disease: practice guidance from the American association for the study of liver diseases. *Hepatology*. 2018;67:328–57.
4. Vuppalanchi R, Noureddin M, Alkhoufi N, Sanyal AJ. Therapeutic pipeline in nonalcoholic steatohepatitis. *Nat Rev Gastroenterol Hepatol*. 2021;18:373–92.
5. Belfort R, Harrison SA, Brown K, Darland C, Finch J, Hardies J, et al. A placebo-controlled trial of pioglitazone in subjects with nonalcoholic steatohepatitis. *N Engl J Med*. 2006;355:2297–307.
6. Sanyal AJ, Chalasani N, Kowdley KV, McCullough A, Diehl AM, Bass NM, et al. Pioglitazone, vitamin E, or placebo for nonalcoholic steatohepatitis. *N Engl J Med*. 2010;362:1675–85.
7. Neuschwander-Tetri BA, Loomba R, Sanyal AJ, Lavine JE, Van Natta ML, Abdelmalek MF, et al. Farnesoid X nuclear receptor ligand obeticholic acid for non-cirrhotic, non-alcoholic steatohepatitis (FLINT): a multicentre, randomised, placebo-controlled trial. *Lancet*. 2015;385:956–65.
8. Food and Drug Administration. Noncirrhotic nonalcoholic steatohepatitis with liver fibrosis: developing drugs for treatment; draft guidance for industry. 2018. p. 62582–3 [cited 2022 Jul 23]. Available from: <https://www.regulations.gov/document/FDA-2018-D-3632-0002>
9. Im YR, Hunter H, de Gracia HD, Duret A, Cheah Q, Dong J, et al. A systematic review of animal models of NAFLD finds high-fat, high-fructose diets most closely resemble human NAFLD. *Hepatology*. 2021;74:1884–901.
10. Santhekadur PK, Kumar DP, Sanyal AJ. Preclinical models of non-alcoholic fatty liver disease. *J Hepatol*. 2018;68:230–7.
11. Ibrahim SH, Hirsova P, Malhi H, Gores GJ. Animal models of nonalcoholic steatohepatitis: eat, delete, and inflame. *Dig Dis Sci*. 2016;61:1325–36.
12. Hebbard L, George J. Animal models of nonalcoholic fatty liver disease. *Nat Rev Gastroenterol Hepatol*. 2011;8:35–44.
13. Farrell G, Schattenberg JM, Leclercq I, Yeh MM, Goldin R, Teoh N, et al. Mouse models of nonalcoholic steatohepatitis: toward optimization of their relevance to human nonalcoholic steatohepatitis. *Hepatology*. 2019;69:2241–57.
14. Dulai PS, Singh S, Patel J, Soni M, Prokop LJ, Younossi Z, et al. Increased risk of mortality by fibrosis stage in nonalcoholic fatty liver disease: systematic review and meta-analysis. *Hepatology*. 2017;65:1557–65.
15. Vilar-Gomez E, Calzadilla-Bertot L, Wai-Sun Wong V, Castellanos M, Aller-de la Fuente R, Metwally M, et al. Fibrosis severity as a determinant of cause-specific mortality in patients with advanced nonalcoholic fatty liver disease: a multi-national cohort study. *Gastroenterology*. 2018;155:443–57.e17.
16. Taylor RS, Taylor RJ, Bayliss S, Hagström H, Nasr P, Schattenberg JM, et al. Association between fibrosis stage and outcomes of patients with nonalcoholic fatty liver disease: a systematic review and meta-analysis. *Gastroenterology*. 2020;158:1611–25.e12.
17. European Medicines Agency. Reflection paper on regulatory requirements for the development of medicinal products for chronic non-infectious liver diseases. 2018.
18. Kleiner DE, Brunt EM, Van Natta M, Behling C, Contos MJ, Cummings OW, et al. Design and validation of a histological scoring system for nonalcoholic fatty liver disease. *Hepatology*. 2005;41:1313–21.
19. Schwartz DM, Wolins NE. A simple and rapid method to assay triacylglycerol in cells and tissues. *J Lipid Res*. 2007;48:2514–20.
20. Caviglia JM, Yan J, Jang M, Gwak G, Affo S, Yu L, et al. MicroRNA-21 and dicer are dispensable for hepatic stellate cell activation and the development of liver fibrosis. *Hepatology*. 2018;67:2414–29.
21. Kennedy AJ, Ellacott KLJ, King VL, Hasty AH. Mouse models of the metabolic syndrome. *Dis Model Mech*. 2010;3:156–66.
22. Okumura K, Ikejima K, Kon K, Abe W, Yamashina S, Enomoto N, et al. Exacerbation of dietary steatohepatitis and fibrosis in obese, diabetic KK-A(y) mice. *Hepatol Res*. 2006;36:217–28.
23. MacKenzie RG. Obesity-associated mutations in the human melanocortin-4 receptor gene. *Peptides*. 2006;27:395–403.
24. Loos RJF. The genetic epidemiology of melanocortin 4 receptor variants. *Eur J Pharmacol*. 2011;660:156–64.
25. Kohli R, Kirby M, Xanthakos SA, Softic S, Feldstein AE, Saxena V, et al. High-fructose, medium chain trans fat diet induces liver fibrosis and elevates plasma coenzyme Q9 in a novel murine model of obesity and nonalcoholic steatohepatitis. *Hepatology*. 2010;52:934–44.
26. Charlton M, Krishnan A, Viker K, Sanderson S, Cazanave S, McConico A, et al. Fast food diet mouse: novel small animal model of NASH with ballooning, progressive fibrosis, and high physiological fidelity to the human condition. *Am J Physiol Gastrointest Liver Physiol*. 2011;301:825–34.
27. Hintze KJ, Benninghoff AD, Cho CE, Ward RE. Modeling the western diet for preclinical investigations. *Adv Nutr*. 2018;9:263–71.
28. Brunt EM, Kleiner DE, Wilson LA, Belt P, Neuschwander-Tetri BA. Nonalcoholic fatty liver disease (NAFLD) activity score and the histopathologic diagnosis in NAFLD: distinct clinicopathologic meanings. *Hepatology*. 2011;53:810–20.
29. Brunt EM. Pathology of fatty liver disease. *Mod Pathol*. 2007;20(Suppl 1):40.
30. Richardson MM, Jonsson JR, Powell EE, Brunt EM, Neuschwander-Tetri BA, Bhathal PS, et al. Progressive fibrosis in nonalcoholic steatohepatitis: association with altered regeneration and a ductular reaction. *Gastroenterology*. 2007;133:80–90.
31. Friedman SL. Hepatic stellate cells: protean, multifunctional, and enigmatic cells of the liver. *Physiol Rev*. 2008;88:125–72.
32. Affo S, Nair A, Brundu F, Ravichandra A, Bhattacharjee S, Matsuda M, et al. Promotion of cholangiocarcinoma growth by diverse cancer-associated fibroblast subpopulations. *Cancer Cell*. 2021;39:866–82.e11.
33. Leung C, Rivera L, Furness JB, Angus PW. The role of the gut microbiota in NAFLD. *Nat Rev Gastroenterol Hepatol*. 2016;13:412–25.
34. Loomba R, Seguritan V, Li W, Long T, Klitgord N, Bhatt A, et al. Gut microbiome-based metagenomic signature for non-invasive detection of advanced fibrosis in human nonalcoholic fatty liver disease. *Cell Metab*. 2017;25:1054–62.e5.

35. Nouredin M, Sanyal AJ. Pathogenesis of NASH: the impact of multiple pathways. *Curr Hepatol Rep*. 2018;17:350–60.
36. Machado MV, Diehl AM. Pathogenesis of nonalcoholic steatohepatitis. *Gastroenterology*. 2016;150:1769–77.
37. Hoang SA, Oseini A, Feaver RE, Cole BK, Asgharpour A, Vincent R, et al. Gene expression predicts histological severity and reveals distinct molecular profiles of nonalcoholic fatty liver disease. *Sci Rep*. 2019;9:12541.
38. Itoh M, Suganami T, Nakagawa N, Tanaka M, Yamamoto Y, Kamei Y, et al. Melanocortin 4 receptor-deficient mice as a novel mouse model of nonalcoholic steatohepatitis. *Am J Pathol*. 2011;179:2454–63.
39. Asgharpour A, Cazanave SC, Pacana T, Seneshaw M, Vincent R, Banini BA, et al. A diet-induced animal model of non-alcoholic fatty liver disease and hepatocellular cancer. *J Hepatol*. 2016;65:579–88.
40. Tsuchida T, Lee YA, Fujiwara N, Ybanez M, Allen B, Martins S, et al. A simple diet- and chemical-induced murine NASH model with rapid progression of steatohepatitis, fibrosis and liver cancer. *J Hepatol*. 2018;69:385–95.
41. Maruvada P, Leone V, Kaplan LM, Chang EB. The human microbiome and obesity: moving beyond associations. *Cell Host Microbe*. 2017;22:589–99.
42. Boursier J, Mueller O, Barret M, Machado M, Fizanne L, Araujo-Perez F, et al. The severity of nonalcoholic fatty liver disease is associated with gut dysbiosis and shift in the metabolic function of the gut microbiota. *Hepatology*. 2016;63:764–75.
43. Tsai M, Liu Y, Lin C, Wang C, Wu Y, Yong C, et al. Gut microbiota dysbiosis in patients with biopsy-proven nonalcoholic fatty liver disease: a cross-sectional study in Taiwan. *Nutrients*. 2020;12:820.
44. Castro RE, Diehl AM. Towards a definite mouse model of NAFLD. *J Hepatol*. 2018;69:272–4.
45. Leclercq IA, Farrell GC, Schriemer R, Robertson GR. Leptin is essential for the hepatic fibrogenic response to chronic liver injury. *J Hepatol*. 2002;37:206–13.
46. Klebig ML, Wilkinson JE, Geisler JG, Woychik RP. Ectopic expression of the agouti gene in transgenic mice causes obesity, features of type II diabetes, and yellow fur. *Proc Natl Acad Sci U S A*. 1995;92:4728–32.
47. Giles DA, Moreno-Fernandez ME, Stankiewicz TE, Graspeuntner S, Cappelletti M, Wu D, et al. Thermoneutral housing exacerbates nonalcoholic fatty liver disease in mice and allows for sex-independent disease modeling. *Nat Med*. 2017;23:829–38.
48. Seki E, De Minicis S, Osterreicher CH, Kluwe J, Osawa Y, Brenner DA, et al. TLR4 enhances TGF-beta signaling and hepatic fibrosis. *Nat Med*. 2007;13:1324–32.

SUPPORTING INFORMATION

Additional supporting information can be found online in the Supporting Information section at the end of this article.

How to cite this article: St. Rose K, Yan J, Xu F, Williams J, Dweck V, Saxena D, et al. Mouse model of NASH that replicates key features of the human disease and progresses to fibrosis stage 3. *Hepatol Commun*. 2022;6:2676–2688. <https://doi.org/10.1002/hep4.2035>